Liquid Metal Embedded Elastomers as Low-BLT Thermal Interface Materials

Dylan Shah, Loren Russell, Keyton Feller, Toby Mea, Navid Kazem
Arieca, Inc
201 N. Braddock Ave, STE 334
Pittsburgh, PA, 15208, USA
Ph: 1 (412) 409 - 9019
Email: navid@arieca.com

Abstract

Thermal interface materials (TIMs) play a critical role in enhancing the efficiency of next-generation packaging technologies within the semiconductor industry. The increasing heat density in the latest transistor node sizes, coupled with increase in die sizes and the prevalence of stacked dies, presents a significant challenge for TIM1s between the die and its heat spreader. Modern TIM1s used in semiconductor packaging must not only offer remarkably low thermal resistances (<5 $mm^2 \cdot K/W$), but also exhibit exceptional mechanical performance to accommodate the significant warpage resulting from coefficient of thermal expansion (CTE) mismatches in the packages.

Recently, researchers have proposed the use of liquid metal embedded elastomers (LMEEs) as thermal interface materials to create a TIM based on LMEEs that can meet the demands of the most challenging applications. In this presentation, we offer material-level characterization and thermal test vehicle (TTV) testing of LMEEs. Our findings demonstrate that achieving an ultra-thin bondline thickness on the order of 20 µm allows us to attain an exceptionally low thermal resistance of less than 5 $mm^2 \cdot K/W$ between the die and integrated heat spreader (IHS).

We provide insights into the interplay between adhesion, stretchability, and modulus of the TIM. These are crucial factors for ensuring the TIM has the necessary mechanical properties to maintain the integrity of the interface between the die and the IHS, thus preventing any degradation in thermal resistance following thermal shock tests. We present data on the in-situ changes in thermal resistance of LMEEs as a function of strain while cured between two copper testheads, shedding light on the thermomechanical behavior of LMEEs. Finally, we conclude by implementing LMEE as the TIM in a TTV package, verifying that the TIM hit the target BLT of 20µm, observable in cross sectional images.

Key words

Liquid Metal, Thermal Interface Material, Semiconductor Packaging, Composite Materials, Thermal Test Vehicle

I. Introduction

The first, and arguably most critical area that heat must pass through when dissipating from high-power-density semiconductors is the thermal interface material (TIM) that adheres the die to its heat spreader, called the TIM1 material. Desirable properties of TIM1 materials include: easy application, low thermal resistance, high electrical resistivity, and thermomechanical robustness, as is typically tested using thermal cycling, bake and highly accelerate stress tests (HAST). Traditional choices of TIM1 include gap fillers (thermal pads), thermal greases, solid TIMs (such as sintered silver and indium alloys), and liquid metals (such as eutectic gallium-indium) [1]. However, as power densities in semiconductor packages have increased dramatically in recent years, thermal engineers are finding it more challenging to obtain TIMs that have suitably low thermal resistance and can survive the required thermal cycling profiles.

Semiconductor assemblies, including at a minimum a silicon die and its packaging, experience fluctuations of warpage during thermal cycling. While this can be partly mitigated through CTE matching throughout the assembly, inevitably, the package will curve, inducing mechanical stress at the interfaces, including the TIM1 (Fig. 1A). For a given mechanical package design, the thermal engineer is tasked with finding a TIM that can fulfill the design's thermal requirements as well as maintaining adhesion during a fixed amount of warpage (w) which we define as the maximum change in BLT experienced in the interface). In turn, the TIM's maximum strain at break (ϵ_m) creates a constraint on the minimum allowable BLT, t_{min} (Fig. 1B). Specifically, minimum BLT $t_{min} = \frac{w}{\epsilon_{break}}$. Thus, in addition to the well-known figure of merit, thermal conductivity κ, and thermal resistance $R_{th} = \frac{t}{\kappa}$, we have found that maximum strain at break (ϵ_m) is a major driver of TIM reliability.

In this paper, we explore how high-elongation liquid metal embedded elastomers (LMEEs) [2] can serve as robust low-BLT thermal interface materials [3]. We begin with mechanical characterization of the standalone TIM, then conduct simultaneous thermo-mechanical testing using an ASTM-D5470 style setup, followed by characterizing the TIM inside of thermal test vehicles. At the end, we discuss open challenges and potential future research directions. This manuscript thus shows key steps toward achieving high-reliability, ultralow BLT thermal interface materials in semiconductor packaging.

A)

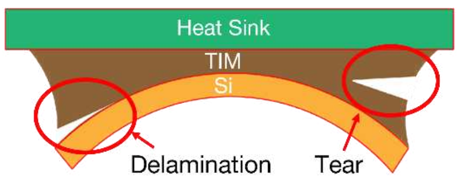

B)

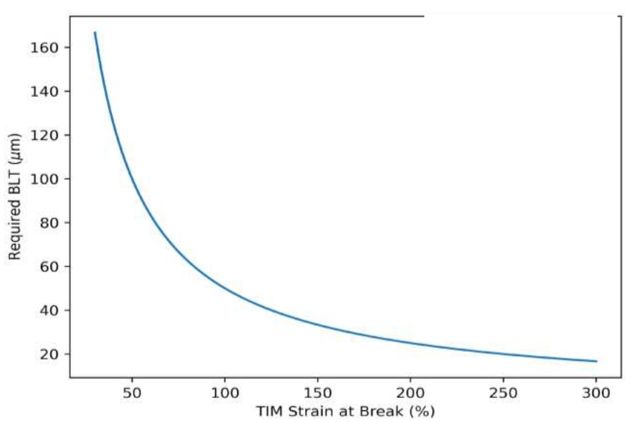

Figure 1. A) During thermal cycling, the TIM experiences mechanical stresses as the heat sink and silicon die warp to different curvatures. This, in turn, leads to delamination. B) TIM strain at break thus dictates a required BLT for mechanical stability. Here, we plot the required BLT as a function of TIM strain at break, in an application where the TIM interface needs to accommodate a warpage-induced elongation of 50 μm.

II. Mechanical Characterization

For this study, we developed a silicone-based polymer that has high strain at break and high adhesion. Using the developed polymer, we fabricated a liquid metal embedded elastomer (LMEE) with high stretchability and adhesion to develop a material for TIM1 that can attain a low BLT. To achieve a feasible material for a TIM1 application, several optimizations were required, but here we will focus on the parameters that are most relevant to obtaining reliable low-BLT TIM interfaces with LMEEs.

Liquid metal droplet size influences the thermal performance and mechanical properties of LMEEs. We fabricated the LMEE with an average droplet size larger than the BLT, to achieve optimal thermal properties [4]. We measured the droplet size of the LMEE using a Ziess optical microscope combined with image-processing software. Next, we evaluated strain at break of the LMEE by stencil-casting dog-bone specimens (500 μm thickness) and stretching them in a materials testing machine (Mark-10 ESM303) at a rate of 50 mm/min, until mechanical failure of the TIM.

The average droplet size of the LMEE was approximately 100 μm in diameter, following a polydisperse distribution (Fig. 2A). This allows each droplet to compress significantly at low BLT (<40 μm), allowing the interfacial thermal resistance to be low. In this study, we were able to achieve LM loading of >60 vol%, without compromising the stretchability of the TIM (Fig. 2B). As the TIM stretched, each liquid metal droplet deformed with its surrounding polymer matrix without rupturing, allowing the TIM to achieve maximum strain at break >350%, with a relatively low elastic modulus of 200-300 kPa.

A)

B)

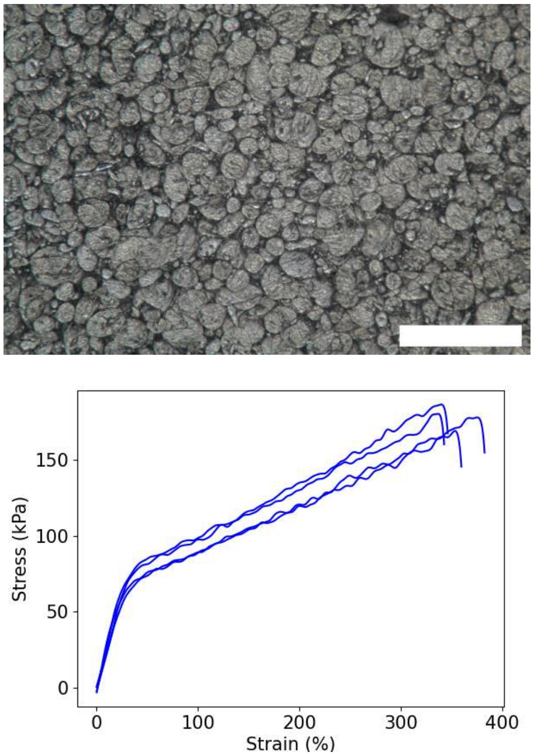

Figure 2. LMEE Characterization. A) microscopy, showing average droplet size ~100 µm. Scale bar is 500 µm. B) uniaxial tensile testing of the LMEE in a stretch-to-failure test. Strain at break typically is in the range of 300-400% (engineering strain).

III. Thermal/Mechanical Characterization

An important criterion for selecting a TIM1 inside semiconductor packaging is the performance during thermal cycling. During the thermal cycling reliability test (JEDEC A106B), the TIM undergoes strain due to changes in the BLT. To simulate the behavior of TIM inside semiconductor packaging, we characterized the LMEE's thermomechanical properties using an ASTM D5470 style test setup (Nanotest, TIMA5; Fig. 3). First, we applied the LMEE in an emulsion state and then compressed it in between two testheads at 20 psi. To maintain a controlled BLT of 20µm throughout the application and curing process, we used two 20µm diameter wires. Next, the upper hot plate and lower cooler temperatures were simultaneously increased to achieve a TIM temperature of 110 °C. We allowed the material to cure under constant pressure of 20 psi for 3 hours. After curing, we reduced the testheads' temperature to allow the temperature of the TIM layer to return to room temperature overnight. Finally, we used the TIMA software to automatically subject the LMEE to repeated strains from ~25% (nominal) to 150% (exact) at a rate of 15 cycles per hour for 50 cycles, while measuring thermal resistance.

When subjected to strains, the thermal resistance increases and decreases in a largely reversible manner (Fig. 4). However, the effective thermal conductivity, measured by calculating BLT/R_{th} (single point effective thermal conductivity) remains consistent at both low and high BLTs (25 µm and 50 µm). Additionally, the TIM returned to the same thermal resistance value when the BLT returned the low end of the cycle, suggesting that the TIM did not delaminate or tear during the mechanical cycles. Delamination or tearing would be detected as higher thermal resistance, since the interfacial thermal resistance would increase due to decreased phonon and electron transport through the introduced air gaps.

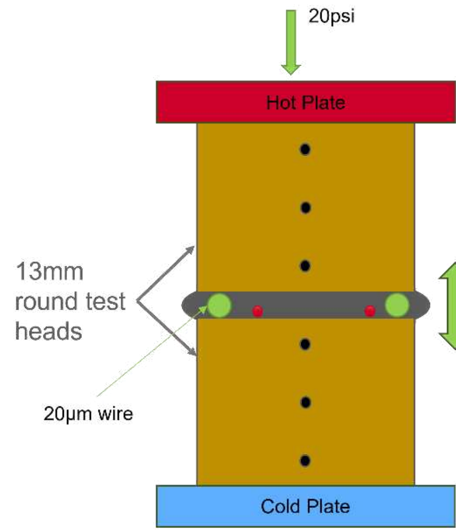

Figure 3. Compressing LMEE in a Nanotest TIMA 5 ASTM D5470 test setup. 20 µm wires were added to ensure a consistent BLT under pressure.

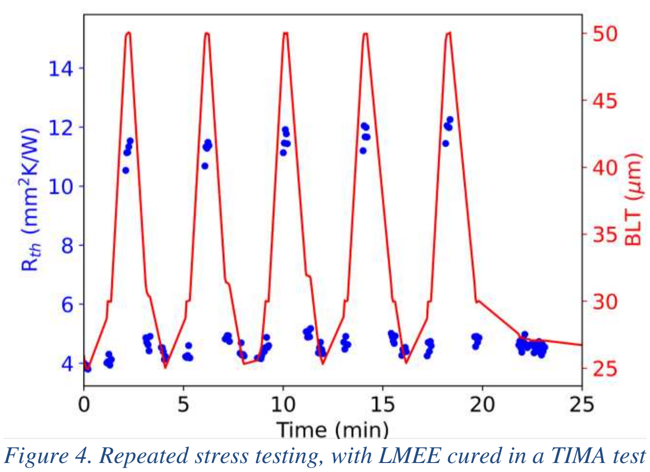

Figure 4. Repeated stress testing, with LMEE cured in a TIMA test setup.

After 50 cycles, the average R_{th} in the low-BLT (unstressed) state remained lower than 5 $mm^2 \cdot K/W$, indicating the TIM maintained its mechanical integrity (Fig. 5). In the future, we plan to quantify the damage profile of the TIM, determining how strain magnitude during cycling affects the thermal resistance and cycles to failure.

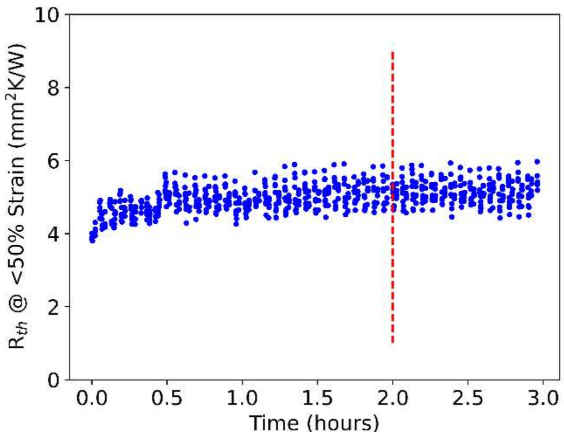

Figure 5. Thermal resistance of LMEE in the low-strain (<50%) portion of multiple cycles from 25% to 150% strain.

IV. Thermal Test Vehicles

The next major evaluation step in a typical TIM qualification process is characterization of the TIM inside semiconductor packaging and evaluating the reliability. To achieve this, we used the same LMEE formulation in a thermal test vehicle (TTV) with a 10 x 10 mm^2 die size (Nanotest NT16-TTV5). The LMEE was pneumatically dispensed onto the die in an X pattern using a CNC dispenser (Fig 6A), followed by dispensing lid sealant (Dowsil SE 4450) along the edge of the lid, and finally a snap cure process where a top heated plate simultaneously applied pressure (40 psi nominal) and heat (150 °C) for 10 minutes to assemble the TTV. The snap cure procedure was followed by an oven cure of 150 °C for 1 hour, to ensure full curing of the lid sealant and the TIM. The thermal resistance of the TIM layer was measured by running the TTV heaters at 10, 20, and 30 W, while simultaneously measuring the die temperature using internal thermistors and measuring the lid temperature using a thermocouple inserted in the lid. For this study, we report the estimated Rth at the corners, center, and average across the die; the reported means and standard deviations are taken across all tested powers to present a conservative uncertainty estimate that is more representative of actual applications (Fig. 6B). Each value was obtained by subtracting the estimates of lid and IHS thermal resistance from the junction-case thermal resistance.

A)

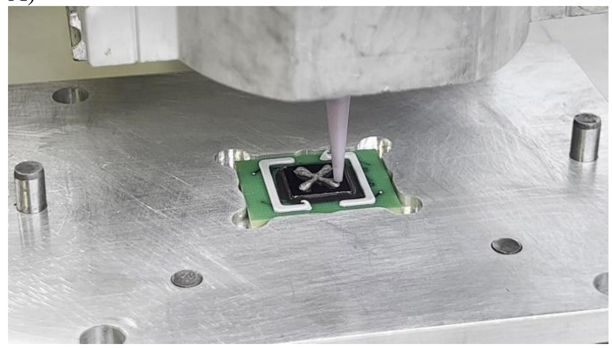

B)

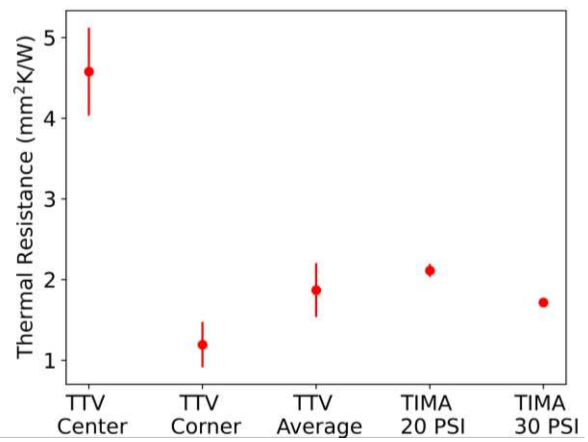

Figure 6. TTV characterization. A) dispensing LMEE onto a TTV die, followed by a TTV snap cure setup. B) Measured R_{th} of LMEE inside of a TTV, using die temperatures at the center and four corners, compared to ASTM D5470 (TIMA5) thermal resistance measurements.

We measured a center R_{th} value of 4-5 mm^2·K/W and an average corner R_{th} (average of four corners) of 1-1.5 mm^2·K/W. We suspect the differences in thermal resistance at the center vs. the corner is either a result of in-plane thermal leakage which results in cooler corner temperatures, or inhomogeneities in the LM distribution after compressing the TIM to low BLT. This will be further investigated using thermal simulations and confocal sound acoustic microscopy (CSAM). Additionally, we compared the average thermal resistance of all 5 TTV measurements (~2 mm^2·K/W) with the thermal resistance measurement obtained using the TIMA5 at 20 psi and 30 psi. We found that the TTV average thermal resistance matched the TIMA thermal resistance values (Fig. 6B).

To confirm the BLT attained in the TTV packaging process, we cross-sectioned a TTV using a diamond saw and diamond polisher (Fig. 7). Interestingly, we did not see evidence of liquid metal alloying the copper, which is common with pure liquid metals. It is hypothesized that the thin elastomer layers encapsulating each liquid metal droplet slows down this process to a negligible rate.

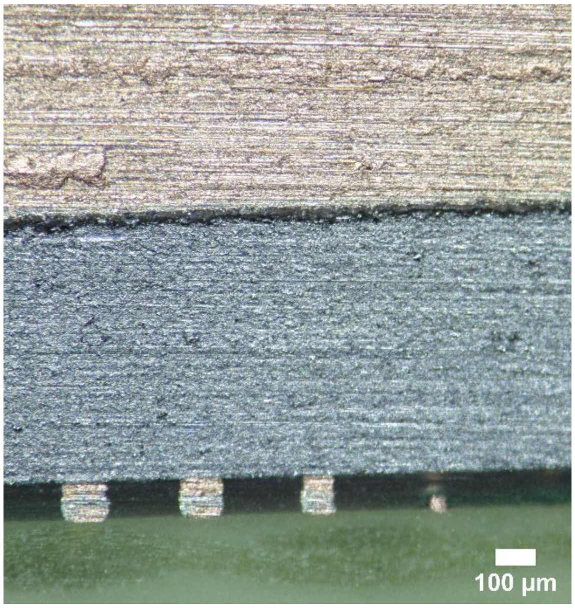

Figure 7. TTV Cross-section. Top to bottom: copper heat spreader, TIM with BLT approximately 20 µm, silicon wafer, underfill and solder bumps, FR4 PCB substrate.

V. Conclusion

This study investigated how LMEE could be adapted to serve low BLT TIM1 semiconductor packaging applications. Specifically, we presented a highly adhesive LMEE that could achieve strains as high as 350% before failure. This gave the TIM a significant safety factor above our experimental stress cycling from 25 to 150% strain, allowing a 20 µm interface to survive cyclic loading with the increase in thermal resistance being approximately 25%. As we moved to TTV characterization, we found that the average thermal performance was similar to results obtained using an ASTM D5470 thermal measurement device. Future investigations include testing with transparent glass test vehicles (replacing the IHS with glass to study the LM distribution throughout the compression cycle) and simulations to investigate the non-uniform thermal resistance, in addition to TTV reliability testing (in particular, thermal shock test).

Acknowledgment

The authors thank Benjamin Dorau for his help developing the LMEE formulations.

References

[1] J. Liu et al., "Recent progress of thermal interface material research - an overview," in 2008 14th International Workshop on Thermal Investigation of ICs and Systems, Sep. 2008, pp. 156–162. doi: 10.1109/THERMINIC.2008.4669900.

[2] N. Kazem, T. Hellebrekers, and C. Majidi, "Soft Multifunctional Composites and Emulsions with Liquid Metals," Advanced Materials, vol. 29, no. 27, p. 1605985, 2017. eprint: https://onlinelibrary.wiley.com/doi/pdf/10.1002/adma.201605985.

[3] M. D. Bartlett, N. Kazem, M. J. Powell-Palm, X. Huang, W. Sun, J. A. Malen, and C. Majidi, "High thermal conductivity in soft elastomers with elongated liquid metal inclusions," Proceedings of the National Academy of Sciences, vol. 114, pp. 2143–2148, Feb. 2017. Publisher: National Academy of Sciences Section: Physical Sciences.

[4] [4] N Kazem, C Majidi - US Patent 10,777,483, 2020